

# EVIDENCE FOR DISTINCT POLYMER CHAIN ORIENTATIONS IN $\text{KC}_{60}$ AND $\text{RbC}_{60}$

P. Launois, R. Moret

*Laboratoire de Physique des Solides (URA CNRS 2), Université Paris-Sud, Bât. 510, 91405 Orsay CEDEX, FRANCE*

J. Hone, A. Zettl

*Department of Physics, University of California at Berkeley,  
and Materials Sciences Division, Lawrence Berkeley National Laboratory, Berkeley, California 94720, USA  
(september 1998: to be published in Phys. Rev. Lett.)*

The  $\text{KC}_{60}$  and  $\text{RbC}_{60}$  polymer phases exhibit contrasting electronic properties while powder diffraction studies have revealed no definite structural difference. We have performed single crystal X-ray diffraction and diffuse scattering studies of these compounds. It is found that  $\text{KC}_{60}$  and  $\text{RbC}_{60}$  possess different chain orientations about their axes, which are described by distinct space groups  $\text{Pmnn}$  and  $\text{I2/m}$ , respectively. Such a structural difference will be of great importance to a complete understanding of the physical properties.

PACS NUMBERS: 61.10.Nz, 61.48.+c

The recently discovered alkali-fullerides  $\text{AC}_{60}$  [1] ( $A=\text{K, Rb, Cs}$ ) exhibit a phase transition from a high temperature cubic phase [2] to an orthorhombic one in which the molecules form one-dimensional polymer chains [3–6], at about  $350\text{K}$ . Despite extensive studies, the physical properties of the latter phase are still the subject of controversy. They have been investigated by ESR [3,7–9],  $\mu\text{SR}$  [10], NMR [8,11–13], and optical and electrical conductivity measurements [7,14].  $\text{RbC}_{60}$  and  $\text{CsC}_{60}$  possess a magnetic transition towards an insulating phase below  $\sim 50\text{K}$ , whereas  $\text{KC}_{60}$  does not. The exact nature of the magnetic low temperature phase is not yet understood; several scenarios for quasi-one-dimensional [3,4,7,9,12] or three dimensional [8,15,16] magnetic ordering are being debated. The different behavior of  $\text{KC}_{60}$  relative to  $\text{RbC}_{60}$  and  $\text{CsC}_{60}$  is also not understood. Recent theoretical calculations show that the chain orientations influence the dimensionality of the electronic properties [17]. However, powder diffraction studies [5] revealed no definite structural difference between  $\text{KC}_{60}$  and  $\text{RbC}_{60}$ . Accordingly, a better knowledge of the details of the  $\text{AC}_{60}$  structures, especially the chain orientations, is needed. We present the first single crystal diffraction study of  $\text{KC}_{60}$  and  $\text{RbC}_{60}$ , and we show that  $\text{KC}_{60}$  and  $\text{RbC}_{60}$  possess different relative chain orientations.

The main structural results [3,5,6] obtained for  $\text{KC}_{60}$  and  $\text{RbC}_{60}$  are summarized in the following. The unit cell is orthorhombic, with parameters  $a$ ,  $b$  and  $c$  equal to 9.11, 9.95, 14.32 Å and to 9.14, 10.11, 14.23 Å for  $\text{KC}_{60}$  and  $\text{RbC}_{60}$ , respectively [5].  $\text{C}_{60}$  molecules are centered at  $(0, 0, 0)$  and  $(1/2, 1/2, 1/2)$  positions, and alkali ions at  $(0, 0, 1/2)$  and  $(1/2, 1/2, 0)$ . Polymerization occurs via [2+2] cycloaddition along the shortest parameter  $a$  (fig.1(a)). The most plausible orthorhombic space groups compatible with the molecular symmetry are  $\text{Immm}$

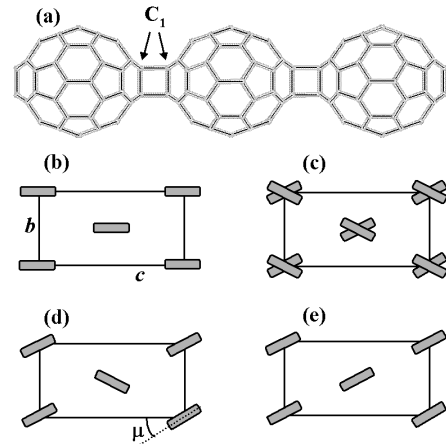


FIG. 1. (a) Linear polymer chain formed by [2+2] cycloaddition. Schematic drawing of chain orientations for (b) ordered  $\text{Immm}$ , (c) disordered  $\text{Immm}$ , (d)  $\text{Pmnn}$ , (e)  $\text{I2/m}$ . The shaded bars indicate the orientation of the polymer chains, they represent the projection of the cycloaddition planes defined by the  $\text{C}_1$  atoms onto the crystallographic (b, c) plane.

and  $\text{Pmnn}$ . The orientation of a  $\text{C}_{60}$  chain about its axis  $\mathbf{a}$  can be characterized by the angle  $\mu$  of the planes of cycloaddition with  $\mathbf{c}$ . For the body-centered space group  $\text{Immm}$ , two configurations must be considered: an ordered one, with  $\mu = 0$  or  $90^\circ$  (fig.1(b)) where chains passing through the origin and the center of the unit cell have the same orientation, and a disordered one if  $\mu \neq 0$  or  $90^\circ$ : the mirror planes perpendicular to  $b$  and  $c$  constrain the chains to take orientations  $\mu$  or  $-\mu$ , with equal probabilities (fig.1(c)). Such a disorder would give rise to diffuse planes perpendicular to  $\mathbf{a}^*$  in reciprocal space. The  $\text{Pmnn}$  structure has glide planes, so that if the orientation of the chain passing through the unit cell origin is  $\mu$ , the orientation of that passing through its center is  $-\mu$  (fig.1(d)). In diffraction,  $\text{Immm}$  can be distinguished

from Pmnn by the extinction of the reflections for  $h+k+l$  odd. From Rietveld refinements, Stephens et al. [5] found  $\mu = 45 \pm 5^\circ$  for both  $\text{KC}_{60}$  and  $\text{RbC}_{60}$  samples, but they could not discriminate between Immm and Pmnn. A pair distribution function analysis performed by Fox et al. [6] indicated a possible orientational chain disorder.

For the present study,  $\text{KC}_{60}$  and  $\text{RbC}_{60}$  crystals (typical size:  $10^{-2} \text{mm}^3$ ) were prepared by stoichiometric doping of  $\text{C}_{60}$  single crystals at  $400^\circ\text{C}$ ; the polymer phase was obtained by subsequent slow cooling (the detailed procedure is described in ref. [14]). The samples were first characterized by X-ray powder diffraction [14](b) and electron beam analysis [18]; their electrical transport properties were reported in ref. [14]. The sample crystallinity suffered from the insertion and polymerization process, but it was still acceptable for our diffraction studies (mosaic spread  $\approx 2^\circ$ , full-width at half-maximum, for  $\text{KC}_{60}$  and  $\approx 2.5^\circ$  for  $\text{RbC}_{60}$ ).

The single-crystal X-ray experiments combined photographic (precession and fixed-crystal) and diffractometer techniques. The precession method, which gives undistorted sections of the reciprocal space, enabled us to check the body-centered extinctions mentioned above and to study the domain structure of the crystal. The latter information cannot be accessed by powder diffraction techniques. The fixed-crystal fixed-film monochromatic technique was employed to detect the X-ray diffuse scattering possibly due to orientational disorder of the  $\text{C}_{60}$  chains. This technique, where the crystal is under vacuum, is particularly efficient as it maximizes the signal/noise ratio. Finally, the diffractometer technique enabled us to make quantitative measurements of the Bragg peak intensities used for structure refinements.

Precession photographs ( $\text{CuK}\alpha$  radiation) have been taken on different crystals to ascertain general results. Complex precession patterns similar to those presented for pressure polymerized  $\text{C}_{60}$  in ref. [19] were obtained. They show the coexistence of orientational variants due to the cubic-orthorhombic symmetry lowering. These variants are related by the lost symmetry operations. We have determined the orientational relationships between the variants, which gives information regarding the structural polymerization mechanism. In  $\text{KC}_{60}$ , the polymerization involves the sliding of dense  $(111)_c$  cubic planes whose orientation is preserved, as in pressure polymerized  $\text{C}_{60}$  [19]. The situation is somewhat different for  $\text{RbC}_{60}$  because the orientation of  $(111)_c$  planes is not preserved. The structural polymerization mechanism observed for pressure polymerized  $\text{C}_{60}$  and for  $\text{KC}_{60}$  does not apply to  $\text{RbC}_{60}$  possibly due to steric constraints imposed by the larger Rb ions. The symmetry elements preserved by the cubic-orthorhombic transformation are (i) in  $\text{KC}_{60}$  the  $[110]_c = \mathbf{b}$  2-fold axis and (ii) in  $\text{RbC}_{60}$  the  $[\bar{1}\bar{1}0]_c = \mathbf{a}$  and the  $[110]_c = \mathbf{b}$  2-fold axes. This transformation generates 12 variants for  $\text{KC}_{60}$  and only 6 for  $\text{RbC}_{60}$ . A careful analysis of the precession patterns

reveals that  $\text{KC}_{60}$  presents a primitive (P) lattice while  $\text{RbC}_{60}$  is body-centered (I, absence of  $h+k+l = 2n+1$  reflections).

Experiments using the fixed-crystal fixed-film method were performed for  $\text{KC}_{60}$  and  $\text{RbC}_{60}$ . They revealed no diffuse scattering. Calculations showed that the diffuse scattering intensity expected for chain disorder should have the same order of magnitude as that produced by the rotating molecules in pure  $\text{C}_{60}$ , which can be easily detected by the fixed-crystal fixed-film method. We thus conclude that the polymer chains are ordered in both  $\text{KC}_{60}$  and  $\text{RbC}_{60}$ .

The Bragg peak intensity measurements on  $\text{KC}_{60}$  and  $\text{RbC}_{60}$  were performed on a three-circle diffractometer, using  $\text{CuK}\alpha$  radiation.  $\text{AC}_{60}$  crystals often present  $\{111\}_c$  twins originating from the parent  $\text{C}_{60}$  crystals and we selected samples with negligible twin volumes ( $\leq 1\%$ ). The unit cell parameters are found equal to those in ref. [5] within experimental accuracy. In order to refine the structure, we had to measure diffraction peaks from a single domain. This task required a selection procedure to exclude overlapping reflections. First we computed the Bragg peak positions for all variants and selected isolated reflections, then we scanned these reflections towards neighboring ones (typically within  $0.8 \text{ \AA}^{-1}$ ), to ensure the absence of contamination. The remaining Bragg peaks were fitted using gaussian profiles, yielding peak intensities  $I_0(hkl)$ . We obtained the following data set of unique and isolated reflections: 177 reflections, among which 107 reflections with  $h+k+l = 2n+1$  and 70 reflections with  $h+k+l = 2n$ , for  $\text{KC}_{60}$ , 82 reflections with  $h+k+l = 2n$  for  $\text{RbC}_{60}$ . Their intensities are relatively weak: only 111 peaks for  $\text{KC}_{60}$  (63 peaks with  $h+k+l = 2n+1$  and 48 peaks with  $h+k+l = 2n$ ) and 39 peaks for  $\text{RbC}_{60}$  verify the relation  $I > \sigma$  [20]. We also checked i) the  $h+k+l = 2n+1$  extinctions for  $\text{RbC}_{60}$ , ii) the glide plane extinctions in  $\text{KC}_{60}$ .

The structural analysis is based on the minimization of the reliability factor [20]

$$R = \sum \left| \frac{|F_{obs}|}{\sum |F_{obs}|} - \frac{|F_{calc}|}{\sum |F_{calc}|} \right| \quad (1)$$

where  $F_{obs}$  and  $F_{calc}$  are observed and calculated structure factors.  $|F_{obs}(h,k,l)|$  is the square-root of the integrated intensity given by  $I = I_0(hkl) \cdot Q^2$  (the mosaic broadening of the reflection is considered to be proportional to  $Q^2$ ), and corrected for polarization effects. The limited intensity data lead us to restrict the number of refined parameters to the chain orientation angle  $\mu$ , an isotropic carbon Debye-Waller (DW) parameter  $U_C$ , anisotropic alkali DW parameters  $U_{11}, U_{22}, U_{33}$ , and the molecular distortion; we relaxed the  $\text{C}_1$  atom positions only, which most affects the reliability factor [5]. We varied these parameters simultaneously over broad ranges using a step by step procedure which required reasonably

small computing times due to the limited data set. The set of parameter values that gave the lowest  $R$  ( $R_{\min}$ ) was retained. In comparison with the usual least-squares refinement method, this procedure enables us to test all possible combinations of the parameters, but its drawback is that uncertainties are not easily evaluated.

The  $R$  values obtained by minimization over the molecular distortion and over the DW factors are plotted versus orientation angle  $\mu$  in fig.2. For Pmnn  $\text{KC}_{60}$ , we obtain  $R_{\min} \simeq 0.16$  for  $U_C \simeq 0.01\text{\AA}^2$ ,  $U_{11}, U_{22}, U_{33} \simeq 0.24, 0.02, 0.3\text{\AA}^2$ ,  $d_{C_1\text{-inter}} \simeq d_{C_1\text{-intra}} \simeq 1.55\text{\AA}$ , and  $\mu \simeq 51^\circ$ . The DW factor for carbon is normal, while those of potassium are unusually large; preliminary experiments as a function of temperature indicate that they probably conceal alkali ion displacements [21].

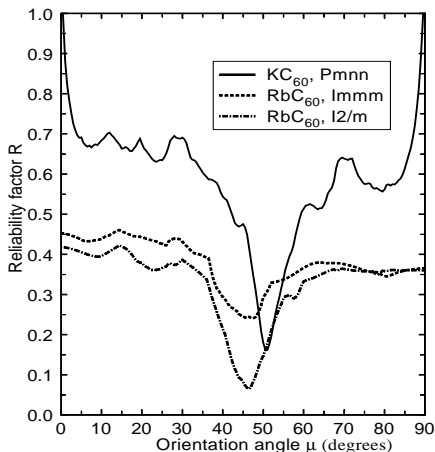


FIG. 2. Reliability factor  $R$  calculated for peaks satisfying  $I > \sigma$ , as a function of the chain orientation  $\mu$  (see the text).

For  $\text{RbC}_{60}$  a refinement was first attempted within the  $\text{Immm}$  space group, leading to  $R_{\min} \simeq 0.24$  for  $\mu \simeq 48^\circ$  (fig.2). However this implies, as indicated before, a  $+\mu/-\mu$  orientational chain disorder which is ruled out by the absence of diffuse scattering. Aside from  $\text{Immm}$ , no body-centered orthorhombic space group is convenient to describe the orientational ordering of  $\text{C}_{60}$  polymer chains. We were thus forced to consider monoclinic body-centered arrangements. The space group compatible with the symmetry of  $\text{C}_{60}$  chains is  $\text{I2/m}$ , with the chain axis parallel to the 2-fold axis; the corresponding chain orientations are depicted in fig.1(e). In this case, the  $(\mathbf{b}, \mathbf{c})$  angle is not constrained to  $90^\circ$ . However, we have not detected a deviation of this angle value from  $90^\circ$  (within an estimated experimental uncertainty of  $0.5^\circ$ ). It may be very weak because of the relatively homogeneous distribution of the atoms on a chain around its axis (if it

were fully homogeneous, the  $(\mathbf{b}, \mathbf{c})$  angle would be equal to  $90^\circ$ ). Within the  $\text{I2/m}$  hypothesis, the reliability factor minimum  $R_{\min} \simeq 0.06$  corresponds to:  $U_C \simeq 0.01\text{\AA}^2$ ,  $U_{11}, U_{33} \simeq 0.16, 0.09 \text{\AA}^2$  [22] ( $U_{22}$  cannot be determined because all measured  $h, k, l$  peaks have small  $k$  values),  $d_{C_1\text{-inter}} \simeq 1.5\text{\AA}$ ,  $d_{C_1\text{-intra}} \simeq 1.6\text{\AA}$ , and  $\mu \simeq 47^\circ$  (fig.2) [23]. This model is highly attractive because the chain orientations are ordered (in agreement with the absence of diffuse scattering) and it greatly improves  $R_{\min}$ , as compared to  $\text{Immm}$ . The chain orientations in  $\text{KC}_{60}$  and  $\text{RbC}_{60}$  ( $\mu \simeq 51^\circ$  and  $47^\circ$ ) are in agreement with the results of Stephens et al. ( $45 \pm 5^\circ$ ) [5], and the molecular distortions are found to be similar in  $\text{KC}_{60}$  and  $\text{RbC}_{60}$  [6]. However the different space groups obtained for  $\text{KC}_{60}$  and  $\text{RbC}_{60}$ , namely  $\text{Pmnn}$  and  $\text{I2/m}$ , imply completely different relative orientations of the chains.

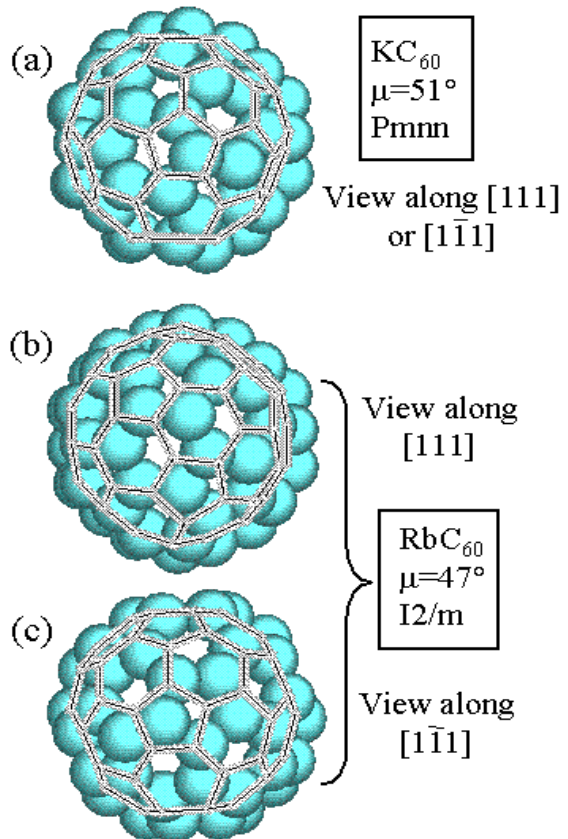


FIG. 3. Molecular environments viewed along the axes  $[111]$  and  $[\bar{1}\bar{1}1]$  joining centers of nearest neighbor molecules in  $\text{KC}_{60}$  and in  $\text{RbC}_{60}$ . The C atoms (spheres) of the more distant molecule are viewed through a portion of the C-C bond skeleton of the nearer one.

It is interesting to compare the structural environments in  $\text{KC}_{60}$  and  $\text{RbC}_{60}$ . The first neighbor  $\text{C}_{60}\text{-C}_{60}$  interchain ( $8.73\text{\AA}$ ) and intermolecular ( $9.85\text{\AA}$ ) distances are remarkably similar for both compounds while the sec-

ond neighbor distance (equal to  $b$ ) increases from 9.95Å (KC<sub>60</sub>) to 10.11Å (RbC<sub>60</sub>). The A-C<sub>60</sub> distance increases for the first neighbors (6.74Å for KC<sub>60</sub> and 6.81Å for RbC<sub>60</sub>) while it decreases slightly for the second neighbors (7.16Å for KC<sub>60</sub> and 7.12Å for RbC<sub>60</sub>). The above distances depend on the unit cell parameters only. The chain orientation comes into play for the interatomic A-C or C-C environments. In both compounds the alkali ions roughly face carbon hexagons from the first neighbors C<sub>60</sub> (along [110] and  $[1\bar{1}0]$ ) and 'single' C-C bonds from their second neighbors (along [001]) [24]. The influence of the different values of  $\mu$  ( $\mu_K \simeq 51^\circ$  and  $\mu_{Rb} \simeq 47^\circ$ ) is small and no clear distinction between KC<sub>60</sub> and RbC<sub>60</sub> can be identified at this point. In contrast the intermolecular C<sub>60</sub> environments are different. There is only one type of environment in KC<sub>60</sub> (along [111] and  $[1\bar{1}\bar{1}]$ ) where a 'double' bond approximately face a pentagon from the neighboring C<sub>60</sub>, as shown in fig.3(a). In RbC<sub>60</sub> the lower space group symmetry implies that the [111] and  $[1\bar{1}\bar{1}]$  intermolecular environments are different, as shown in fig.3(b) and (c). It is possible that alkali-C<sub>60</sub> interactions favor roughly the same chain orientation angle in KC<sub>60</sub> and RbC<sub>60</sub> ( $\sim 45 - 50^\circ$ ), while the C<sub>60</sub>-C<sub>60</sub> interactions determine the relative chain orientations and thus the space group symmetry. Preliminary calculations [21] have indeed shown that the C<sub>60</sub>-C<sub>60</sub> intermolecular potential varies appreciably with the chain orientations, the symmetry of their arrangement and the unit cell parameters. This should be kept in mind when analyzing pressure effects and pressure induced transitions in AC<sub>60</sub> compounds [8,14,25].

MAS-NMR spectra of RbC<sub>60</sub> and CsC<sub>60</sub> are very similar and differ from that of KC<sub>60</sub> [11,13]. Alloul et al. [11] suggested that the distribution of spin density along a chain is influenced by its neighbors. With the present results, we can now attribute the difference between the KC<sub>60</sub> and RbC<sub>60</sub> spectra to the distinct relative chain orientations in the two compounds (fig.1(d) and (e)). The similarity of the RbC<sub>60</sub> and CsC<sub>60</sub> spectra suggests that the chain orientations are likely the same in RbC<sub>60</sub> and CsC<sub>60</sub>. As discussed in the introduction, the physical properties of RbC<sub>60</sub> and CsC<sub>60</sub> are very similar and differ markedly from those of KC<sub>60</sub>. A strong correlation between physical properties and relative chain orientations can thus be inferred in polymerized AC<sub>60</sub>. Electronic structure calculations have already been performed by Erwin et al. [15] and by Tanaka et al. [17] for I2/m RbC<sub>60</sub>. Further theoretical investigations taking into account the distinct chain orientations in AC<sub>60</sub> are much awaited.

#### ACKNOWLEDGMENTS

J.H. and A.Z. acknowledge support from the U.S. Department of Energy under Contract No. DE-AC03-76SF00098.

- 
- [1] J. Winter and H. Kuzmany, Solid State Comm. **84**, 935 (1992).
  - [2] Q. Zhu et al., Phys. Rev. B **47**, 13948 (1993).
  - [3] O. Chauvet et al., Phys. Rev. Lett. **72**, 2721 (1994).
  - [4] S. Pekker et al., Solid State Comm. **90**, 349 (1994).
  - [5] P.W. Stephens et al., Nature **370**, 636 (1994).
  - [6] J.R. Fox et al., Chem. Phys. Lett. **249**, 195 (1996).
  - [7] F. Bommeli et al., Phys. Rev. B **51**, 14794 (1995).
  - [8] P. Auban-Senzier et al., J. Phys. I France **6**, 2181 (1996).
  - [9] A. Jánossy et al., Phys. Rev. Lett. **79**, 2718 (1997).
  - [10] Y.J. Uemura et al., Phys. Rev. B **52**, 6991 (1995); W.A. MacFarlane et al., Phys. Rev. B **52**, 6995 (1995); L. Cristofolini et al., J. Phys.: Condens. Matter **7**, L567 (1995).
  - [11] H. Alloul et al., Phys. Rev. Lett. **76**, 2922 (1996); V. Brouet et al., in *Molecular Nanostructures*, H. Kuzmany et al. Ed., World Scientific, 1998, p.328.
  - [12] V. Brouet et al., Phys. Rev. Lett. **76**, 3638 (1996).
  - [13] F. Rachdi et al., Appl. Phys. A **64**, 295 (1997).
  - [14] (a) J. Hone et al., Phys. Rev. B **52**, 8700 (1995); K. Khazeni et al., Phys. Rev. B **56**, 6627 (1997); (b) K. Khazeni et al., Appl. Phys. A **64**, 263 (1997).
  - [15] S.C. Erwin, G.V. Krishna and E.J. Mele, Phys. Rev. B **51**, 7345 (1995).
  - [16] H. Kuzmany et al., Physica B **244**, 186 (1998).
  - [17] K. Tanaka et al., Chem. Phys. Lett. **272**, 189 (1997).
  - [18] N.G. Chopra, J. Hone and A. Zettl, Phys. Rev. B **53**, 8155 (1996).
  - [19] R. Moret et al., Europh. Lett. **40**, 55 (1997); P. Launois et al., in *Molecular Nanostructures*, H. Kuzmany et al. Ed., World Scientific, 1998, p. 348.
  - [20] G.H. Stout and L.H. Jensen, *X-ray diffraction structure determination, a practical guide*, John Wiley & Sons, Inc., 1989.
  - [21] P. Launois et al., Proceedings of the 1998 International Conference on Science and Technology of Synthetic Metals, to appear in *Synthetic Metals*.
  - [22] The DW values may be slightly underestimated since the data were not corrected for absorption.
  - [23] In principle the monoclinic distortion should lead to more than 6 orientational variants. However the distortion is not observed within the resolution of the present study, and its effect can be safely neglected. We also mention that we have assumed equivalent domains with chain orientations  $\mu$  and  $-\mu$  to calculate the structure factors  $F_{calc}$ .
  - [24] In the usual C<sub>60</sub> nomenclature, 'single' C-C bonds fuse a hexagon and a pentagon and 'double' C-C bonds fuse two hexagons.
  - [25] B. Simovic et al., to appear in the Proceedings of the Kirchberg Conference, 1998.